

Superior glass-forming ability through microalloying in cerium-based alloys

B. Zhang, R. J. Wang, D. Q. Zhao, M. X. Pan, and W. H. Wang*
Institute of Physics, Chinese Academy of Sciences, Beijing 100080, China
 (Received 25 November 2005; published 2 March 2006)

We find that minute trace addition (as low as 0.2 at. %) can dramatically enhance glass-forming ability in a simple cerium-based alloy, accompanied by a fragile-to-strong transition and markedly structural and properties changes. The phenomena, which cannot be explained well by often-cited theories and empirical rules for metallic glass formation, are attributed to an increase of the short-range ordering in the alloys. The results provide evidences for the close relation among the liquid fragility, glass-forming ability, and structure in glass-forming alloys and may assist in understanding the long-standing issue on glass formation.

DOI: [10.1103/PhysRevB.73.092201](https://doi.org/10.1103/PhysRevB.73.092201)

PACS number(s): 61.43.Dq, 61.25.Mv, 81.05.Kf, 64.70.Kb

Due to the considerable scientific and technological importance of bulk metallic glasses (BMGs),¹⁻³ a large number of efforts have been devoted to investigate the glass-forming ability (GFA) of metallic alloys in order to develop new BMGs with superior GFA. A few theoretical and empirical criteria based on structure, thermodynamics, and kinetics have been proposed.¹⁻⁵ However, the understanding of the mechanisms of glass formation, which is a very complex phenomenon that has defied rigorous scientific understanding, still remains a challenge and the application of BMGs is impeded by their low GFA.¹⁻³

Recently, it was found that the fragility m [an index of how fast the viscosity increases while approaching the structural arrest at glass transition temperature, T_g (Ref. 6)] is empirically correlated with other properties.⁷⁻¹³ For example, m is related to the mean-square displacement, the configuration entropy, and even the relative strength of shear and bulk moduli of the corresponding glass.¹¹ The correlation found implies that the factors that determine the nature of a glass-forming system could have a close relation with its liquid behavior, and the answer for an underlying mechanism for the glass formation might be buried deep in the liquid. Tanaka¹⁴ found a correlation between short-range ordering and fragility, i.e., the stronger tendency of short-range ordering in stronger glass formers. In fact, some excellent BMG-forming alloys have been found to be strong glass formers.¹³ On the other hand, efforts have been made to explore the glass-forming issue on a structural point of view. A model for metallic glasses was proposed that emphasizes the importance of efficient packing of atoms into clusters and provides a way for understanding short- and medium-range order in metallic glasses and allows predictions of new glass-forming alloy composition.⁵ Thus, it would be important to study the glass formation combining with the liquid behavior and structural features of the alloys.

In this work, we find that a superior GFA in a simple ternary $\text{Ce}_{70}\text{Al}_{10}\text{Cu}_{20}$ alloy ("matrix alloy" in the following context) can be induced by minute trace microalloying, which cannot be explained well by the often-cited theories and empirical rules for BMG formation. We have investigated the changes of the liquid behavior and structure and find that a fragile-to-strong transition and markedly structural and elastic properties changes accompany the dramatically enhanced GFA in the Co microalloyed alloys. It is assumed

that the existence of strong-bonding local structure induced by microalloying changes the liquid nature through increasing the short-range ordering and thus slows down crystallization kinetics on cooling.

The ingots of $\text{Ce}_{70-x}\text{Al}_{10}\text{Cu}_{20}\text{Co}_x$ ($0 \leq x \leq 5$ at. %) were prepared by arc melting the mixtures of pure Ce, Al, Cu, and Co elements in argon atmosphere. The ingots were remelted and sucked into a copper mold to get cylindrical samples. The structure of the samples was analyzed with x-ray diffraction (XRD) using a MAC M03 XHF diffractometer (Cu- K_α radiation) and differential scanning calorimeter (DSC) using a Perkin-Elmer DSC7. The acoustic velocities (v_l and v_s) were measured using a pulse echo overlap method by a MATEC 6600 model ultrasonic system.³ The density was determined by the Archimedeian principle and the accuracy lies within 0.1%. The Young's modulus E , shear modulus G , bulk modulus K , Poisson's ratio σ , and Debye temperature θ_D were derived from the density and acoustic velocities¹⁵ as follows: $G = \rho v_s^2$; $K = \rho(v_l^2 - 4/3v_s^2)$; $\sigma = \rho(v_l^2 - 2v_s^2)/2(v_l^2 + v_s^2)$; $E = 2G(1 + \sigma)$. θ_D at room temperature can also be represented as:¹⁵

$$\theta_D = \frac{h}{k_B} \left(\frac{4\pi}{9} \right)^{-1/3} \rho^{1/3} \left(\frac{1}{v_l^3} + \frac{2}{v_s^3} \right)^{-1/3},$$

where k_B is the Boltzmann constant, h the Planck constant, and ρ the density.

Figure 1(a) exhibits the pictures of the Ce-based BMG rods. The lustrous surfaces of the BMGs indicate that they have good castability upon solidification. Figure 2 exhibits XRD patterns for the as-cast alloys. The matrix alloy ($x = 0$) with 2 mm in diameter and Co microalloyed alloys ($x = 0.2, 0.5, 1, \text{ and } 2$) with 8–10 mm in diameter show similar broad diffused diffraction maximum ($2\theta \approx 32^\circ$) with an average d value of $2.78 \pm 0.05 \text{ \AA}$, which demonstrating the typical amorphous structure of these samples. The XRD pattern of the matrix alloy with diameter $\phi = 5 \text{ mm}$ is also presented and exhibits apparent crystalline peaks of the cubic Ce, AlCe_3 , and other unknown compounds, demonstrating that its GFA is much lower than that of the microalloyed alloys. The critical diameter (d_c) of the alloys as a function of Co addition is illustrated in Fig. 1(b). With minute traces of Co addition (0.2%) d_c is dramatically increased from 2 mm to at

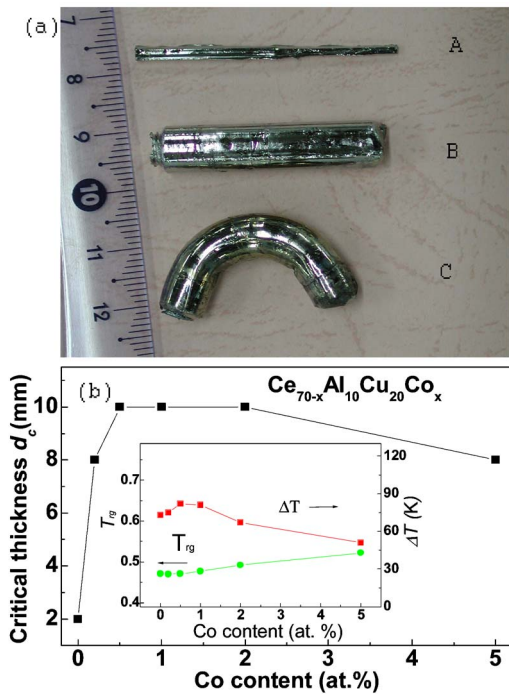


FIG. 1. (Color online) (a) Picture of the matrix $Ce_{70}Al_{10}Cu_{20}$ BMG bar ($\phi=2$ mm) (A) and $Ce_{69.8}Al_{10}Cu_{20}Co_{0.2}$ BMG rod ($\phi=8$ mm) in as-cast state (B) and $Ce_{68}Al_{10}Cu_{20}Co_2$ BMG rod in shaped form (C) bent by hand in near-boiling water. (b) The relation between the critical diameter (d_c) and Co content. A sharp increase of d_c with 0.2% Co microalloying is shown, and the inset shows the changes of T_{rg} and ΔT as a function of Co microalloying content.

least 8 mm. The effective Co addition for improving GFA is below 2%. Such a sensitive change of GFA resulting from microalloying of transition metal is in contrast to the previous findings that the beneficial addition is usually $>2\%$.¹⁶ The approach should be applicable to a variety of systems and would assist in guiding BMG development by selection of proper microalloying elements.

The typical DSC traces of these alloys are exhibited in Fig. 3. The distinct glass transition and sharp crystallization confirm the glassy structure of these alloys. The exceedingly low T_g (below 100 °C) with a large supercooled liquid region, ΔT_x of these BMGs makes it possible to observe the intrinsic viscous behavior of the supercooled liquid near am-

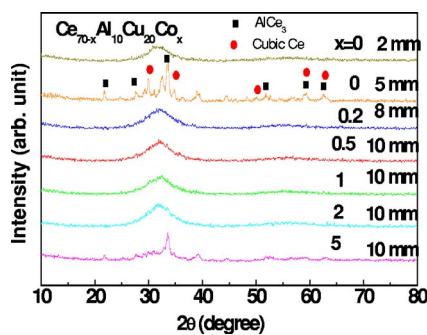


FIG. 2. (Color online) XRD patterns for the matrix alloy and Co microalloying alloys.

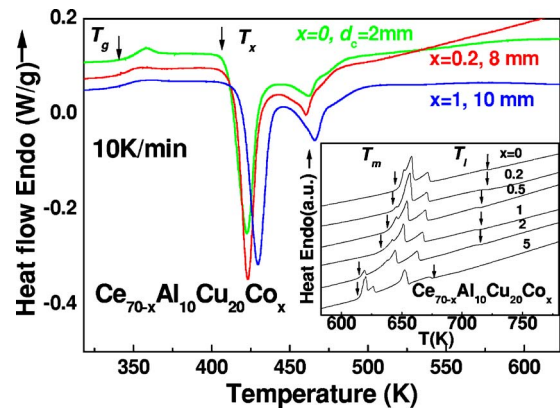


FIG. 3. (Color online) Typical DSC traces focusing on the glass transition and crystallization for the $Ce_{70-x}Al_{10}Cu_{20}Co_x$ ($x=0, 0.2,$ and 1) BMGs (the heating rate is 10 K/min). The inset shows the melting events of the $Ce_{70-x}Al_{10}Cu_{20}Co_x$ alloys at the same heating rate.

bi-ent temperature. For example, the 8-mm-diameter BMG bar can be hand shaped in near-boiling water [see Fig. 1(a)]. In near-boiling water, these materials can also be repeatedly shaped similar to polymeric thermoplastic, and can thus be regarded as metallic plastics. Such a perfect superplasticity in near-boiling water, which is not expected in the crystalline alloys, indicates some potential applications. The T_g , crystallization temperature T_x , $\Delta T(=T_x - T_g)$, liquidus temperature T_l , and reduced glass transition temperature, $T_{rg} = T_g/T_l$, of these alloys are listed in Table I. ΔT and T_{rg} , which are often used parameters in evaluating the GFA of an alloy, do not reflect the significant changes of the GFA of the alloys [see the inset of Fig. 1(b)]. Although Co microalloying actually decreases T_l , as shown in the inset of Fig. 3, such a superior GFA cannot be attributed to the deep eutectic effect, which is efficient in many other BMGs.¹⁻³ Previous work suggests that good GFA consistent with forming BMGs is associated with $T_{rg} \geq 0.6$,² while these alloys do not show expected larger T_{rg} . Figure 4 shows the critical cooling rate (R_c) as a function of T_{rg} for various glasses.¹⁷⁻¹⁹ The T_{rg} of the alloys is close to that of Al-based (0.45, Ref. 19) and Pd-Si (0.48, Ref. 18) melt-spun glasses that show poor GFA. Consequently, the T_{rg} and ΔT criteria cannot explain the remarkably large GFA in the alloys. The dramatic effect on GFA cannot be explained by “confusion theory”¹ and the atomic

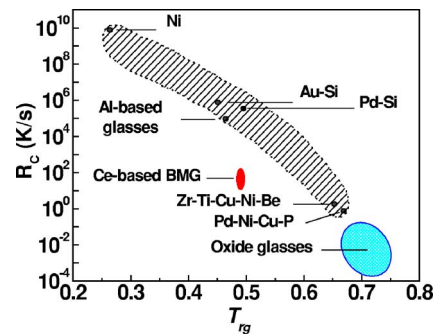


FIG. 4. (Color online) The relation between T_{rg} and critical cooling rate R_c for various glasses.

TABLE I. The critical thickness d_c and the thermal parameters of T_g , T_x , ΔT , T_l , and T_{rg} for the matrix and Co microalloyed alloys.

Alloys (at. %)	d_c (mm)	T_g (K)	T_x (K)	ΔT (K)	T_l (K)	T_{rg} (T_g/T_l)
Ce ₇₀ Al ₁₀ Cu ₂₀	2	337	410	73	722	0.471
Ce _{69.8} Al ₁₀ Cu ₂₀ Co _{0.2}	8	339	414	75	721	0.470
Ce _{69.5} Al ₁₀ Cu ₂₀ Co _{0.5}	10	337	419	82	716	0.471
Ce ₆₉ Al ₁₀ Cu ₂₀ Co ₁	10	340	421	81	713	0.477
Ce ₆₈ Al ₁₀ Cu ₂₀ Co ₂	10	352	419	67	716	0.492
Ce ₆₅ Al ₁₀ Cu ₂₀ Co ₅	8	345	414	69	676	0.510

size factor either (Co and component Cu have similar atomic size).

To understand the underlying mechanism for such an unusual phenomenon, we investigate the fragility of these alloys. The liquid fragility can be determined in a purely thermodynamic way near T_g , and the m estimated this way are consistent with those obtained by kinetic method.^{12,20} Because the increase on reheating of the heat capacity from glass value to equilibrium liquid value occurs over a range of temperature and the range is determined by how quickly the relaxation time changes with temperature, a correlation of fragility with the reduced glass transition width $\Delta T_g/T_g$ ($\Delta T_g = T_{g-end} - T_g$) from DSC scan has been demonstrated for glasses, which is closely related to the thermodynamic fragility $F_{1/2}$.²⁰ The correlation can be used to monitor the colorimetric fragility change of the microalloyed alloys. As shown in the inset of Fig. 5, the Ce₆₉Al₁₀Cu₂₀Co₁ BMG has a large $\Delta T_g/T_g$ (0.074) (other Co microalloyed BMGs

have similar $\Delta T_g/T_g$ values and all larger than that of the silica-based glass NBS711), while the matrix alloy has low value of $\Delta T_g/T_g$ (0.041) close to that of the typical fragile liquid of propylene carbonate. A combination of these results and various glasses¹² is shown in Fig. 5 (details are presented in the Fig. 5 legend), and the $\Delta T_g/T_g$ values for the BMGs are marked by the horizontal dashed arrows. One can see that a distinct “fragile”-“strong” transition occurs and the fragile matrix liquid is converted to more strong liquid by traces of Co microalloying. The transition is also supported by the jump in apparent heat capacity (ΔC_p) near T_g . A small jump in ΔC_p near T_g suggests a strong resistance to structural degradation in a liquid, e.g., strong liquids such as SiO₂ show a small jump near T_g in ΔC_p while the typical fragile liquids such as AuPbSb alloy²¹ and propylene glycol show a sharp peak or large ΔC_p jump.⁶ The ΔC_p upon glass transition versus T_g -scaled temperature is plotted in the inset of Fig. 5. Apparently, the Co bearing alloys exhibit different C_p changes near T_g and the ΔC_p “jump” is much smaller compared with that of the matrix alloy. When ΔC_p is very small, the configuration entropy S_c [$S_c = \int (\Delta C_p/T) dt$] is almost T independent, and then the Adam-Gibbs equation²² [$\tau = \tau_0 \exp(A/TS_c)$, where τ is relaxation time, τ_0 and A are constants] would predict an Arrhenius temperature dependence of relaxation behavior corresponding to a strong liquid. The correlation of a small value of m with a small jump in ΔC_p upon glass transition conforms that the chemical manipulations of the alloy, by minute traces of Co addition, can convert “fragile” liquid into intermediate strong liquid when vitrified at T_g accompanying with dramatically increase of

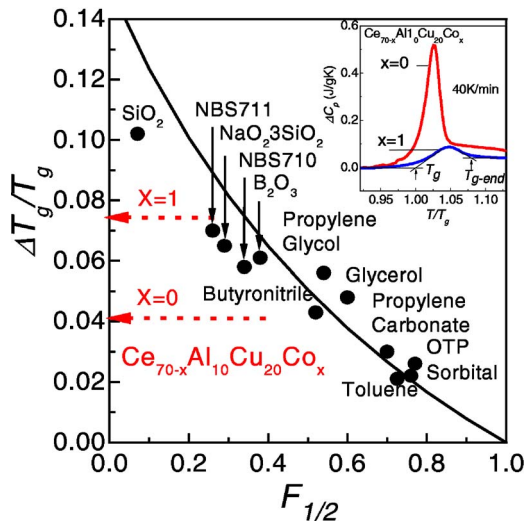


FIG. 5. (Color online) Relation between $\Delta T_g/T_g$ and $F_{1/2}$. $\Delta T_g/T_g$ has been demonstrated to correlate with the fragility parameter $F_{1/2}$ for inorganic and molecular glasses as a VFT function (the solid line) (Ref. 12). We use this correlation to determine the fragility for the present BMGs, and the dashed arrows to the vertical axis show the $\Delta T_g/T_g$ of Ce_{70-x}Al₁₀Cu₂₀Co_x ($x=0$ and 1) BMGs, which is defined and determined from the T_g -scaled DSC curves at 40 K/min in the inset. The fragility plots (the filled circle) for the inorganic and molecular glasses are taken from Ref. 12.

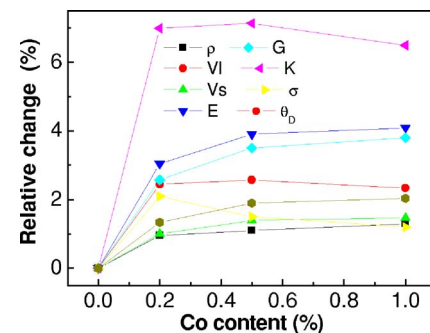


FIG. 6. (Color online) Relative changes of the density, elastic moduli, and Debye temperature for the Co microalloyed BMGs with respect to the matrix BMG as a function of Co content.

TABLE II. The density ρ , longitudinal (v_l) and transverse (v_s) acoustic velocities, elastic constants (E , G , K , and σ), and Debye temperature θ_D for the glassy matrix and Co microalloyed alloys.

Alloys (at. %)	ρ (g/cm ³)	v_l (km/s)	v_s (km/s)	E (GPa)	G (GPa)	K (GPa)	σ	θ_D (K)
Ce ₇₀ Al ₁₀ Cu ₂₀	6.669	2.568	1.296	29.91	11.25	29.18	0.329	142.3
Ce _{69.8} Al ₁₀ Cu ₂₀ Co _{0.2}	6.733	2.631	1.309	30.82	11.54	31.22	0.336	144.2
Ce _{69.5} Al ₁₀ Cu ₂₀ Co _{0.5}	6.744	2.634	1.314	31.08	11.64	31.26	0.334	145.0
Ce ₆₉ Al ₁₀ Cu ₂₀ Co ₁	6.753	2.628	1.315	31.13	11.68	31.07	0.333	145.2

GFA. The superior GFA of the alloys correlates with the strong liquid behavior, which has also been reported in other BMGs.^{13,23–25}

To find out possible structural origins of the transition, the elastic properties measured by acoustic method, which is useful for probing subtle structural changes, are investigated.¹⁵ The density, acoustic velocities, elastic constants, and Debye temperature for the amorphous alloys are collected in Table II. The changes of density, elastic moduli, and Debye temperature relative to the matrix alloy are contrasted in Fig. 6. The relative density increases 0.95%, 1.1%, and 1.3% for 0.2%, 0.5%, and 1% Co microalloyed BMGs, respectively. All the acoustic velocities and elastic moduli show abrupt change for the alloy with 0.2% Co alloying. For example, the relative changes of v_l and K are close to the changes induced by full crystallization in other BMGs (in Zr-based BMG, the crystallization induced relative changes of v_l and K are 5.2% and 3.9%, respectively³). A sharp increase of θ_D is also induced by 0.2% Co addition; the distinct increase of θ_D means the acoustic modes in the alloys with Co addition become much stiffer compared with the matrix Co free alloy. The results demonstrate that the fragile-to-strong transition accompanies sudden structural and properties changes. The much more dense packing structure and the markedly properties change are the signature of the existence of some especially strong bonds in the alloys.¹⁵

The degree of short-range ordering in a liquid controls the fragility, and the stronger tendency of short-range ordering in a stronger glass former.¹⁴ Thus the decrease of m and the higher degree of atomic packing imply a strong tendency of short-range ordering in the microalloyed alloys. The strong glass formers usually have a covalent tetrahedral network with stable short- and medium-range structure. Generally, the degree of short-range bond ordering increases in the covalent-bonded liquids, and network-forming covalent liquids such as SiO₂ are typically strong glass formers.⁶ The local strong ordering structure plays the key role in the glass formation. The structural ordering leads to a decrease of S_c of the liquid. According to the Adam-Gibbs theory,²² this will result in more viscous and higher density liquid that slows down the crystallization kinetics on cooling and then enhances the GFA of the alloys. Fe element was reported to show strong covalent bonding with Al in the Al-Fe-Ce metallic glasses.²⁶ Fe microalloying has been performed and a similar effect on the GFA of the Ce-based matrix alloy has been found.

The support of the Natural Science Foundation of China (No. 50321101, No. 503711097 and No. 503711098) and the Chinese Academy of Sciences (No. KGX2-SW-214-1) is appreciated.

*Contacting author. Email address: whw@aphy.iphy.ac.cn

¹A. L. Greer, *Science* **267**, 1947 (1995).

²A. Inoue, *Acta Mater.* **48**, 279 (2000).

³W. H. Wang, C. Dong, and C. H. Shek, *Mater. Sci. Eng., R.* **44**, 45 (2004).

⁴D. Turnbull, *Contemp. Phys.* **10**, 473 (1969).

⁵D. B. Miracle, *Nat. Mater.* **3**, 697 (2004).

⁶C. A. Angell, *Science* **267**, 1924 (1995).

⁷L.-M. Martinez and C. A. Angell, *Nature (London)* **410**, 663 (2001).

⁸J. C. Dyre and N. B. Olsen, cond-mat/1211042 (unpublished).

⁹S. Sastry, *Nature (London)* **409**, 164 (2001).

¹⁰T. Scopigno, *Science* **302**, 849 (2003).

¹¹V. N. Novikov and A. P. Sokolov, *Nature (London)* **431**, 961 (2004).

¹²K. Ito, C. T. Moynihan, and C. A. Angell, *Nature (London)* **398**, 492 (1999).

¹³R. Busch, E. Bakke, and W. L. Johnson, *Acta Mater.* **46**, 4725 (1998).

¹⁴H. Tanaka, *Phys. Rev. Lett.* **90**, 055701 (2003).

¹⁵D. Schreiber, *Elastic Constants and Measurement* (McGraw-Hill, New York, 1973).

¹⁶W. H. Wang, Y. Zhang, M. X. Pan, and D. Q. Zhao, *Intermetallics* **10**, 1249 (2002).

¹⁷H. J. Fecht and W. L. Johnson, *Mater. Sci. Eng., A* **375–377**, 2 (2004).

¹⁸Z. P. Lu and C. T. Liu, *Acta Mater.* **50**, 3501 (2002).

¹⁹F. Q. Guo, S. J. Poon, and G. J. Shiflet, *Scr. Mater.* **43**, 1089 (2000).

²⁰C. T. Moynihan, *J. Am. Ceram. Soc.* **76**, 1081 (1993).

²¹H. J. Fecht, *Mater. Trans., JIM* **36**, 777 (1995).

²²G. Adam and J. H. Gibbs, *J. Chem. Phys.* **43**, 139 (1965).

²³L. Shadowspeaker and R. Busch, *Appl. Phys. Lett.* **85**, 2508 (2004).

²⁴J. M. Borrego, W. Loeser, and J. Eckert, *J. Appl. Phys.* **92**, 2073 (2002).

²⁵D. V. Louzguine, S. Sobu, and A. Inoue, *Appl. Phys. Lett.* **85**, 3758 (2004).

²⁶H. Y. Hsieh and W. L. Johnson, *J. Mater. Res.* **5**, 2807 (1990).